ISTP

RESEARCH ARTICLE

An Improved Dynamic Modelling for Exploring Ball Bearing Vibrations from Time-Varying Oil Film

Minmin Xu,[1] **Zhenzhen Song,**[1] **Xiaoxi Ding,**[1] **Guoxing Li,**[2] **Yimin Shao,**[1] **and James Xi Gu**[3]

[1]State Key Laboratory of Mechanical Transmission, Chongqing University, Chongqing 400044, China
[2]College of Mechanical and Vehicle Engineering, Taiyuan University of Technology, Taiyuan 030024, China
[3]School of Engineering, University of Bolton, Bolton, BL3 5AB, UK

Abstract: Bearings are key components in rotating machinery, which is widely used in many fields, such as CNC machines, wind turbines and induction machines. The increasingly harsh operation environment can lead to wear and tear on raceways and reduce the precision and reliability of bearing or even machinery. Lubrication could relieve the wear to some degree, which is benefit to prolong the bearing's life. Thus, investigation on the vibration responses under the influence of oil film is of great significance. However, for mechanism analysis, how to include the oil film into the bearing dynamic model affects the result and efficiency of solution. To address this problem, this study proposed a fast algorithm through load distribution and interpolation when calculating oil film stiffness and thickness during the solution of bearing vibration model. Analysis of oil film on vibration is carried out and a bearing test rig is designed to verify the proposed model. Numerical simulation result shows that rotational speed and load have vital effect on oil film and vibration. The experimental result is consistent with the simulation, which shows that the proposed model has a better performance on modeling bearing vibration and the method of considering oil film is reasonable.

Key words: dynamic modeling; fault diagnosis; lubrication; rolling elements bearing; time-varying oil film

I. INTRODUCTION

Bearing is a significant part in rotating machinery, which is commonly used in many fields, such as wind turbine, CNC machine tool, automobile, airplane and precision equipment [1,2,3]. With the development and requirement of mechanical transmission equipment towards to high power density and large-scale, the working environment of bearing has become more complicated and harsh, resulting in wear and high probability of failure on bearing, which lead to low precision and reliability of mechanical equipment. Investigation has shown that 30% fault is result from bearing in rotating machinery. If the infant fault can be detected at an early stage, timely maintenance can be arranged to avoid catastrophic accidents and reduce economic loss. Therefore, the fault diagnosis of bearing is of great significance to the actual application and production.

Vibration signal has been proven to be an effective source data for fault diagnosis. Modelling the bearing vibration through dynamics models and analysing the responses based on the model solution is widely adopted when the mechanism is not revealed or incomplete. During the operation of rolling elements bearings, wear and skidding is inevitable, which reduce the service time of bearing. Fortunately, lubrication could relieve the wear to some degree, which is benefit to prolong the bearing's life. Thus, how to include the oil film into the bearing vibration model to investigate its vibration characteristics is of great significance. To address this problem, considerable research works can be found in literature.

To study the dynamic behaviours of bearings, Harris [4,5] investigated skidding behavior in roller and ball bearings through a quasi-static analytical method. Gupta [6] established a ball bearing dynamic model to investigate the transient motion of rolling element. Meeks and Tran [7] investigated the ball and cage motions in time domain through an analytical ball bearing dynamics model. Cao et al. [8] reviewed five kinds of rolling bearing models for bearing vibration response analysis. Liu et al. [9,10,11] proposed various dynamic models for bearing systems considering the influences of localized defect on raceways, additional deformations at the sharp edges and waviness. Xu et al. [12,13] have investigated the effect of bearing clearances on vibration characteristics for condition monitoring through vibration models. However, the oil film is neglected in these works.

Considering the of oil film, elastohydrodynamic lubrication (EHL) is an effective tool to study its characteristics. Wijnant et al. [14] established the dynamic model of the rolling bearing under the action of elastic lubrication, and studied the effect of the contact angle on the characteristic frequency. Sarangi et al. [15] studied the dynamics of elastohydrodynamic mixed lubricated ball bearings, including the stiffness and damping. In another work [16], nonlinear structural vibration was analysed through a vibration model. Zhang et al. [17] developed the instantaneous EHL model and vibration model to study the dynamic behavior of the rolling bearings, and improved the calculation efficiency by using a discrete and fast Fourier transform method to obtain the relationship between the oil membrane stiffness and the load and velocity. Hajishafiee et al. [18] described a new described a new methodology focus on computational fluid dynamics for modelling elastohydrodynamic contacts. Cui et al. [19] investigated the thermal elastohydrodynamic lubrication (TEHL) analysis of a deep groove ball bearing.

_____
Corresponding author: Prof. Yimin Shao (e-mail: ymshao@cqu.edu.cn)

Bizarre et al. [20] formulates the force and moments equilibrium of an angular contact ball bearing accounting for stiffness and damping under the effects of the EHL. Wu et al. [21] studied the kinetic characteristics of angular contact ball bearing and reveals the influence of structural parameters of rolling bearing on bearing contact and lubrication performance. However, the iteratively solving process of EHL in vibration model is time-consuming and difficult to converge, due to that the oil film thickness and stiffness, contact force and bearing deformation change with time.

To address this problem, corrected formula proposed by Hamrock and Dowson is widely used to describe the characteristics of oil film. Sharad Jain and Hugh Hunt [22] proposed a dynamic model to study the bearing skidding using EHL theory. Zhang et al. [23] established a bearing stiffness matrix under the action of ejection lubrication and compared the difference in the stiffness coefficient under the lubrication and dry contact conditions. Liu et al. [24] proposed an analytical model for roller bearing, in which the lubricated races was taken into account. Han et.al [25] investigated the skidding behavior of cylindrical roller bearings considering Hertz contact theory and EHL. Shi [20] proposed an improved bearing vibration model to investigate the responses of a cylindrical roller bearing, in which oil film stiffness was included. But in these studies, the thickness and stiffness of the oil film was usually regarded as a constant. The time-varying characteristics were neglected, which reduce the accuracy of the vibration model. However, during the operation, the oil film will change with time due to the dynamic force and motion of the components. Thus, how to take into account the characteristics of the time-varying oil film with high accuracy and efficiency is a problem needs to be addressed and it is of great significance for bearing vibration analysis and fault diagnosis.

In this study, an improved bearing dynamic modelling method considering the influences of oil film is introduced and a fast calculation method for the oil film thickness and stiffness is adopted throughout the numerical solving process of the model based on load distribution and interpolation. The rest of the paper is arranged as follow. Section II expounds the time-varying oil film and detailed process of the bearing dynamic model. The implementation of the numerical simulation is presented in Section III, and the result and discussions are carried out in Section IV. Section V validates the vibration model through a bearing test rig.

II. TIME-VARYING OIL FILM AND ITS NUMERICAL SOLVING IN BEARING VIBRATION MODEL

A. THICKNESS AND STIFFNESS OF OIL FILM

When bearing is lubricated during operation, rolling elements and raceways are separated by oil film, which can avoid direct contact between the two surfaces and relieve the bearing wear to prolong the bearing's rotating life. EHL is formed and point contact EHL occurs in ball bearing. Due to that the contact areas are much smaller than the radius of raceways and balls, the contact can be regards as a contact between an elastomer with the radius R_x and a rigid plane. The equivalent elastomer moves towards the rigid plane under the action of the normal load N. Oil film is compressed and deformed in the contact area. As an elastic fluid,
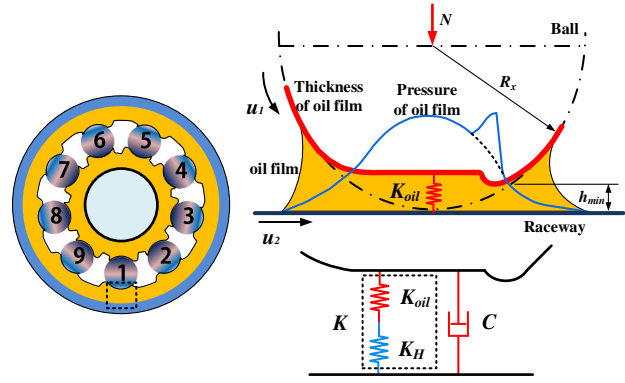

Fig. 1. Thickness and Stiffness of oil film.

the oil film between the two contacts is equivalent to a massless spring element, as shown in Fig. 1.

The equivalent spring consists of the series of bearing and oil film, and the equivalent contact stiffness and damping coefficient can be calculated as [12,13,26].

$$1/K = 1/K_{oil} + 1/K_T \tag{1}$$

$$C = 2\varsigma\sqrt{m_b \times K} \tag{2}$$

where K_{oil} is the stiffness of oil film, K_T is the Hertz contact stiffness, which can be calculated through Refs. [12,27], ς is the damping ratio and m_b is the mass of each ball. Note that an equivalent total damping coefficient is adopted for simplifying the problem of the time-varying characteristic resulted from oil film.

According to EHL theory, the flow of the oil can be obtained by Reynolds equation. The Elliptical contact 2 Dimension isothermal EHL Reynolds equation is given as [19]

$$\frac{\partial}{\partial x}\left(\frac{\rho h^3}{\eta}\frac{\partial p}{\partial x}\right) + \frac{\partial}{\partial y}\left(\frac{\rho h^3}{\eta}\frac{\partial p}{\partial y}\right) = 12u_e\frac{\partial(\rho h)}{\partial x} \tag{3}$$

$$h = h_0 + \frac{x^2}{2R_x} + \frac{y^2}{2R_y} + \frac{2}{\pi E}\iint_\Omega \frac{P(s,t)}{\sqrt{(x-s)^2+(y-t)^2}}dsdt \tag{4}$$

where p and h is the pressure and thickness of the oil film, respectively, x and y is the coordinates along the circumferential and width directions of the bearing, respectively. u_e is the entrainment speed of lubricant, ρ and η is the density and viscosity of lubricant, h_0 is the initial thickness of the lubricant, R_x and R_y denotes the composite radius along x and y direction, respectively, E is the Poisson's ratio, Ω is fluid dimensionless computational area, s and t is the additional coordinates on the x and y axis, respectively.

The thickness and pressure of the oil film will reach a stable state during the solution, as shown in Fig. 2. The normal stiffness of the oil film can be obtained by

$$K_{oil} = \frac{\Delta F_n}{\Delta x_n} = \frac{A \times \sum_{i=1}^M \sum_{j=1}^M \Delta p_{ij}(t)}{\frac{1}{MN}\sum_{i=1}^M\sum_{j=1}^N \Delta h_{ij}(t)} \tag{5}$$

where ΔF_n and Δx_n stands for the increment of contact force and oil film deformation, A is area of the cell grid, M and N is the size of the cells in X and Y direction, respectively.
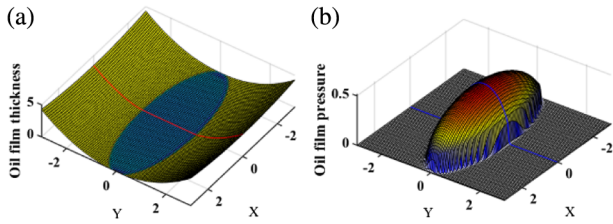
Fig. 2. EHL numerical solution result: (a) Dimension oil film thickness and (b) pressure.

However, the solution process of vibration responses is time-consuming and difficult to converge, due to that the oil film thickness h and stiffness K, deformation δ and contact force N change with time during the solution, as shown in Fig. 3(a). Besides, if the oil film is regarded as a constant, as shown in Fig. 3(b), it will neglect the time-varying characteristics of oil film and reduce the accuracy of the vibration model.

B. FAST METHOD FOR NUMERICAL SOLVING CONSIDERING OIL FILM

To solve these problems, an improved bearing vibration model is proposed and a fast method is adopted by load distribution and interpolation when calculating oil film stiffness and thickness at a certain instant during the solution process of the vibration model, as shown in Fig. 4.

In the proposed method, the oil film thickness and stiffness is considered to have reached a stable state and can be obtained by Hamrock and Dowson empirical formula [28], which is proposed to calculate the dimensionless minimum oil film thickness and oil film stiffness for elliptical contact EHL.

$$h_{\min}^{i,o} = 3.63\bar{U}_{i,o}^{0.68}\overline{G}^{0.49}\overline{W}^{-0.073}\left(1 - e^{-0.68k}\right)R_x \quad (6)$$

$$K_{oil}^{i,o} = \frac{dF}{dh_{\min}^{i,o}} = 6.4066 \times 10^8 h_{\min}^{-14.6986}\bar{U}^{9.3157}\overline{G}^{6.7123}$$
$$E'R_x^{15.6986}\left(1 - e^{-0.68\,k}\right)^{15.6986} \quad (7)$$

Where G is the dismensionless material parameter, $\overline{U}$ is the dimensionless velocities parameter [27,28]
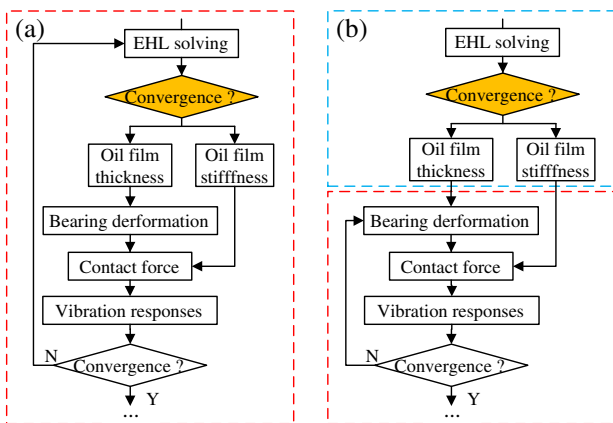

Fig. 3. Numerical solving methods: (a) EHL solving is inside bearing vibration solving and (b) Oil film is a constant.
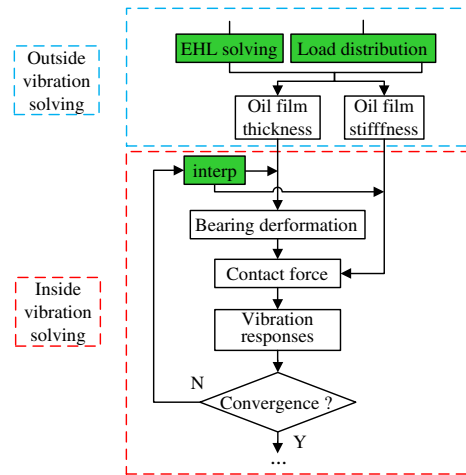

Fig. 4. The proposed method.

$$\bar{U} = \frac{\eta_0 U_{i,o}}{2E'R_x} \quad (8)$$

η_0 represents the original dynamic viscosity of the lubricating oil. $U_{i,o}$ is the lubricant roll suction speed between the rolling elements and the inner and outer races. For the contact area between the rolling elements and the inner/outer ring [27]

$$U_i = \frac{d_m}{2}\left[(1-\gamma)\left(w_i - w_{bo}\right) + \gamma w_{bs}\right] \quad (9)$$

$$U_o = \frac{d_m}{2}\left[(1+\lambda)w_{bo} + \gamma w_{bs}\right] \quad (10)$$

where d_m is pitch diameter, γ is the parameters equals to d_b/d_m, w_i is the angle velocity of the inner race, w_{bo} and w_{bs} is the orbital angle velocity and self-rotating angle velocity of each ball, respectively.

In Eq. (4) and Eq. (5), $\overline{W}$ is dimensionless load parameter

$$\overline{W} = \frac{W}{ER_x^2} \quad (11)$$

where W is the load, R_x is the equivalent radius of curvature between the rolling elements and raceways.

To include the time-varying characteristics of the oil film into vibration model with sufficient accuracy and high efficiently, load distribution is introduced, which is given as [24,27]:

$$W(\psi) = k_r(\psi)F_R$$
$$= \frac{\left(1 - \left(1 + \frac{c}{2\delta_0}\right)\left(1 - \cos\psi\right)\right)^{\frac{3}{2}}}{\frac{z}{2\pi}\int_{-\psi_0}^{\psi_0}\left(1 - \left(1 + \frac{c}{2\delta_0}\right)\left(1 - \cos\psi\right)\right)^{\frac{3}{2}}\cos\psi d\psi}F_R \quad (12)$$

where c is bearing clearance, δ_0 stands for the contact deformation caused by acting of external load on a place of the most loaded ball "0"-rolling element, ψ_0 is equal to π, ψ denotes the integral angle interval, F_R represents the external load, z is the total number of rolling element.

Taking bearing 6206 under the rotational speed of 1500 rpm and external load of 500 N as an example, the thickness and stiffness of the oil film between a ball and
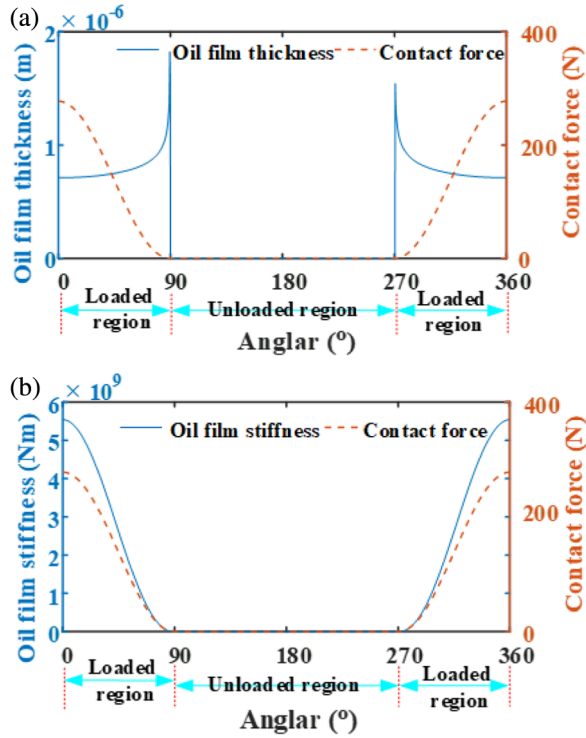
(a)

(b)

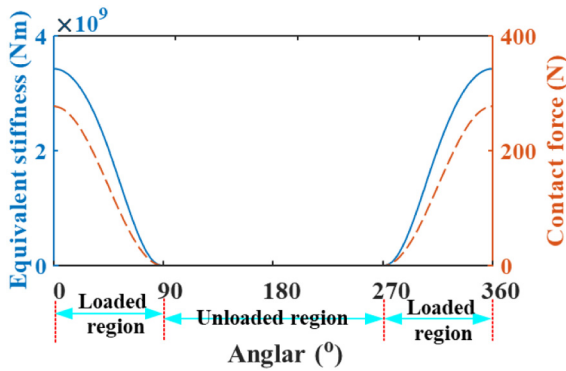**Fig. 5.** Oil film: (a) thickness in a cycle and (b) stiffness in a cycle.

Fig. 6. Equivalent contact stiffness in a cycle.

raceway during a cycle are shown in Fig. 5. It can be find that the thickness and stiffness of the oil film fluctuate with the contact force in the loaded region. The larger force applied between the ball and raceway in the loaded region, the thinner oil film thickness and the lager oil film stiffness. In the unloaded region, the contact force is zero, leading to zero oil film thickness and stiffness.

The equivalent contact stiffness can be calculated by Eq. (1) and is shown in Fig. 6. The equivalent contact stiffness shows similar wave with stiffness of oil film but with lower amplitude due to series in Eq. (1).

C. NONLINEAR BEARING DYNAMIC MODEL

To investigate the vibration response of bearings, a dynamic model is established with 13 DOF, as shown in Fig. 7, in which motion of shaft, housing and balls are included.
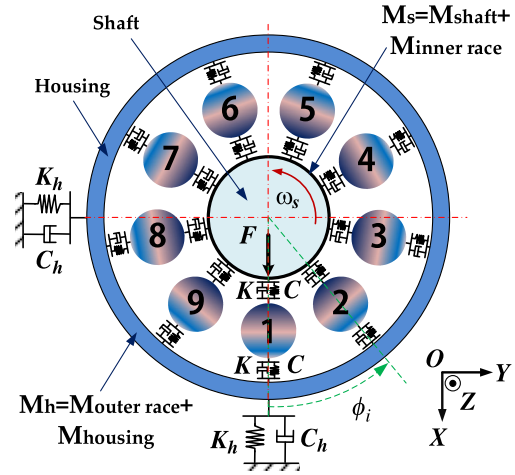

Fig. 7. Bearing dynamic model.

The shaft-bearing-housing model is given in Eqs. (13,14,15,16,17).

$$M_s\ddot{X}_s + K_sX_s + C_s\dot{X}_s + N_{sbx} + F_{fsbx} - G_s = F \quad (13)$$

$$M_s\ddot{Y}_s + K_sY_s + C_s\dot{Y}_s + N_{sby} - F_{fsby} = 0 \quad (14)$$

$$M_h\ddot{X}_h + K_hX_h + C_h\dot{X}_h - N_{bhx} - F_{fbhx} - G_h = 0 \quad (15)$$

$$M_h\ddot{Y}_h + K_hY_h + C_h\dot{Y}_h - N_{bhy} + F_{fbhy} = 0, \quad (16)$$

$$M_b\ddot{r}_i - N_{sbi} + N_{bhi} - F_{ri} - G_b\cos\phi_i = 0, i = 1,2,\ldots,N_b \quad (17)$$

where $\ddot{X}_i/\dot{X}_i/X_i$ denotes the acceleration/ velocity/ displacement, the subscript $i = s,h$ means shaft (s) and housing (h). M_s, M_h and M_b denotes the mass of shaft, housing and ball, respectively. G_s, G_h and G_b means the force of gravity. K_s and K_h represents the stiffness of shaft and housing, while C_s, C_h is the damping. $N_{sbx,y}$ means the resultant contact force between shaft and balls in X and Y direction, $N_{bhx,y}$ means the resultant contact force between balls and housing in X and Y direction. Similarly, $F_{fsbx,y}$ and $F_{fbhx,y}$ means the resultant friction force. N_{sbi} denotes the contact force between the inner race and i^{th} balls, while N_{bhi} means the contact force between the ith balls and outer race. r_i and F_{ri} denotes the radial displacement and centrifugal force of the ith ball, respectively.

$$N_{sbx} = \sum_{i=1}^{N_b} N_{sbi}\cos\phi_i; F_{fsbx} = \sum_{i=1}^{N_b} -\mu N_{sbi}\cos\phi \quad (18)$$

$$N_{sby} = \sum_{i=1}^{N_b} N_{sbi}\sin\phi_i; F_{fsby} = \sum_{i=1}^{N_b} -\mu N_{sbi}\sin\phi \quad (19)$$

$$N_{bhx} = \sum_{i=1}^{N_b} N_{bhi}\cos\phi_i; F_{fbhx} = \sum_{i=1}^{N_b} -\mu N_{bhi}\cos\phi \quad (20)$$

$$N_{bhy} = \sum_{i=1}^{N_b} N_{bhi} \sin \phi_i; \quad F_{fbhy} = \sum_{i=1}^{N_b} -\mu N_{bhi} \sin \phi \quad (21)$$

$$N_{sbi} = F_{ssbi} + F_{dsbi} = K_i \delta_{sbi}^{1.5} + C_i v_{sbi} \quad (22)$$

$$N_{bhi} = F_{sbhi} + F_{dbhi} = K_o \delta_{bhi}^{1.5} + C_o v_{bhi} \quad (23)$$

$K_{i,o}$ and $C_{i,o}$ respectively denotes the stiffness and damping coefficient between inner/outer raceways and balls. δ_i and v_i denotes the nonlinear deformation and velocity of ith ball, respectively; ϕ_i denotes the current angle position of the ith ball, N_b is the total number of balls, c is the bearing clearance,

Considering the time-varying oil film thickness, the deformation δ_i and v_i can be given as

$$\delta_{sbi} = \begin{cases} X_s \cos \phi_i + Y_s \sin \phi_i - r_i - c/4 + h_{\min}^i; & \delta_{sbi} > 0; \\ 0, & \delta_{sbi} \le 0, \end{cases}$$
$$(24)$$

$$\delta_{bhi} = \begin{cases} r_i - X_h \cos \phi_i - Y_h \sin \phi_i - c/4 + h_{\min}^o, & \delta_{bhi} > 0; \\ 0, & \delta_{bhi} \le 0. \end{cases}$$
$$(25)$$

$$v_{sbi} = \begin{cases} \dot{X}_s \cos \phi_i + \dot{Y}_s \sin \phi_i - \dot{r}_i, & \delta_{sbi} > 0 \\ 0, & \delta_{sbi} \le 0 \end{cases} \quad (26)$$

$$v_{bhi} = \begin{cases} \dot{r}_i - \dot{X}_s \cos \phi_i - \dot{Y}_s \sin \phi_i, & \delta_{bhi} > 0; \\ 0, & \delta_{bhi} \le 0. \end{cases} \quad (27)$$

Note that $h_{min}^{i,o}, \delta_{sbi}, \delta_{bhi}, K_{i,o}$ and $C_{i,o}$ have time-varying characteristics.

III. NUMERICAL SIMULATION

A. PARAMETERS

In the simulation study, deep groove ball bearing. 6206 is taken as an instance. The main physical and geometry parameters adopted in the bearing model are listed in Tables I and II.

B. ALGORITHM

Figure 8 depicts the flow path of the numerical solution for the vibration model. A fast solving algorithm through interpolation is adopted. The thickness and stiffness in one cycle are calculated beyond the numerical solving according to load distribution and EHL. The relationship of thickness and stiffness related to angle can be obtained.

Table I   Physical properties in simulation

Notation	Description	Value
m_s	Mass of shaft (kg)	1.32
m_h	Mass of housing (kg)	0.46
m_b	Mass of each ball (kg)	2.95×10^{-3}
K_h	Stiffness of house (N/m)	1.2×10^9
C_h	Damping of house	939.62

Table II   Geometry parameters in simulation

Notation	Description	Value
d	Diameter of nominal bore (mm)	30
D	Diameter of nominal outside (mm)	62
d_i	Diameter of inner raceway (mm)	37.47
d_o	Diameter of outer raceway (mm)	56.46
d_m	Pitch diameter (mm)	46.97
d_b	Ball diameter (mm)	9.482
c	Original radial clearance (μm)	20
N_b	Number of rollers	9
α	Contact angle (°)	0
E	Elastic modulus (GPa)	207
ν	Poisson ratio	0.3

The dynamic model is solved at different time, which can be transformed into angle. Thus, at different angle, the thickness and stiffness of oil film can be obtained through interpolation. The detailed solving process can be divided into 5 steps, as shown in Table III.
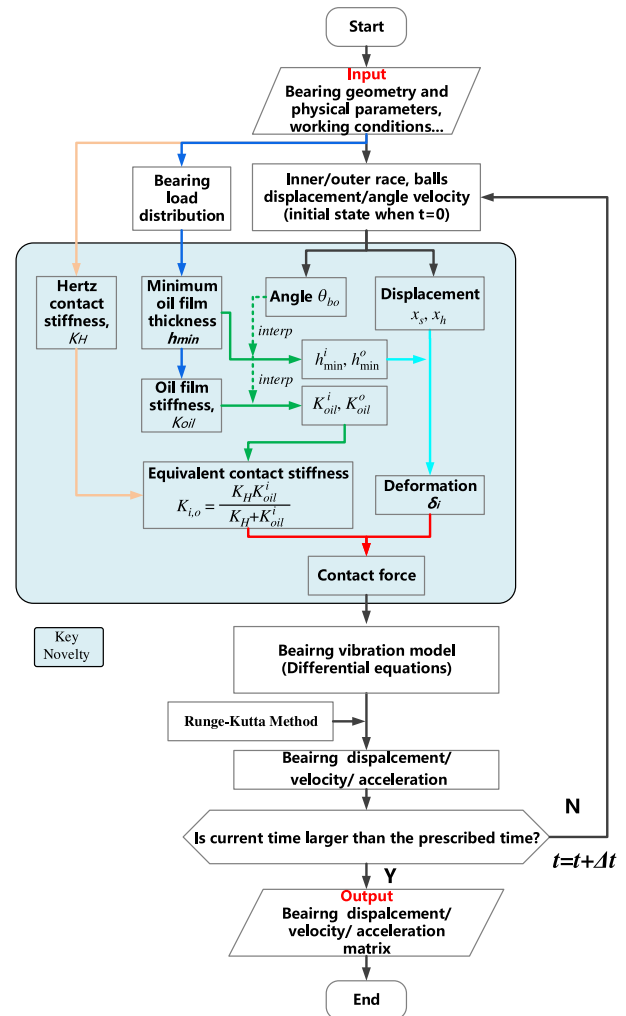

Fig. 8. Flowchart of the calculation process.

Table III   Main steps of the adopted algorithm

Step	Operation
1	input parameters, such as geometry and physical parameters, working conditions and set initial values of the parameters need to solve before the numerical iterative solution.
2	calculate load distribution by Eq. (12) and time-varying oil film thickness and stiffness by Eqs. (6–11).
3	obtain oil film thickness and stiffness at a certain instance through interpolation.
4	Calculate the deformation, contact force and friction force by Eqs. (18–27).
5	Solve the equations with Runge-Kutta method until the prescribed time and output the result.

IV. RESULTS AND DISCUSSIONS

A. EFFECTS OF OIL FILM ON VIBRATION RESPONSES

To study the influence of oil film on bearing vibration, a comparison is carried out among between without oil film and with oil film. In addition, two different methods for simulating oil film are also compared, i.e., simulation method of constant oil film and the proposed time-varying oil film. Vibration responses form time domain and frequency domain are analyzed, as shown in Figs. 9 and 10.

Figure 9 depicts the vibration waveform of the inner race and outer race on X direction. Form Fig. 9, when oil film is taken in account, the vibration is lower on amplitude than without oil film from time domain waveform. Specially, vibration form time-varying oil is lower than constant oil film.

Figure 10 depicts the FFT spectrum and envelope spectrum of the outer race. The Characteristic frequencies of bearing6206 are shown in Table IV, including rotating frequency, ball pass frequency on outer race (BPFO), ball pass frequency on outer race (BPFI), ball spin frequency (BSF) and cage frequency (CF).

Form Fig. 10, two resonant peak can be seen in the FFT spectrum, i.e., 717.8 Hz and 8077 Hz. At low frequency band, there is no sideband. However, on two side of high frequency band, sideband can be detected. Form the envelope spectrum, whether considering oil film or not, the bearing characteristic frequency BPFO is dominant, which means that the ball pass through the outer race plays a vital effect on bearing vibration. This can be attributed to the dynamic contact forces between the balls and outer raceway. As can be seen from Fig. 11, the contact force shows impulsive waveform during the operation. There are nine impulses during a cycle (0.1002 s) and there will be about 89.8 balls passing a same place on outer raceway in one second, which is consistent with the value of BPFO.

When oil film is taken in account, the vibration is lower on amplitude than without oil film from frequency amplitude. Specially, vibration form time-varying oil is lower than constant oil film.

B. INFLUENCES OF SPEED AND LOAD ON OIL FILM AND VIBRATION RESPONSES

The oil film stiffness and oil film thickness caused by rotating speed, bearing load and dynamic viscosity of oil
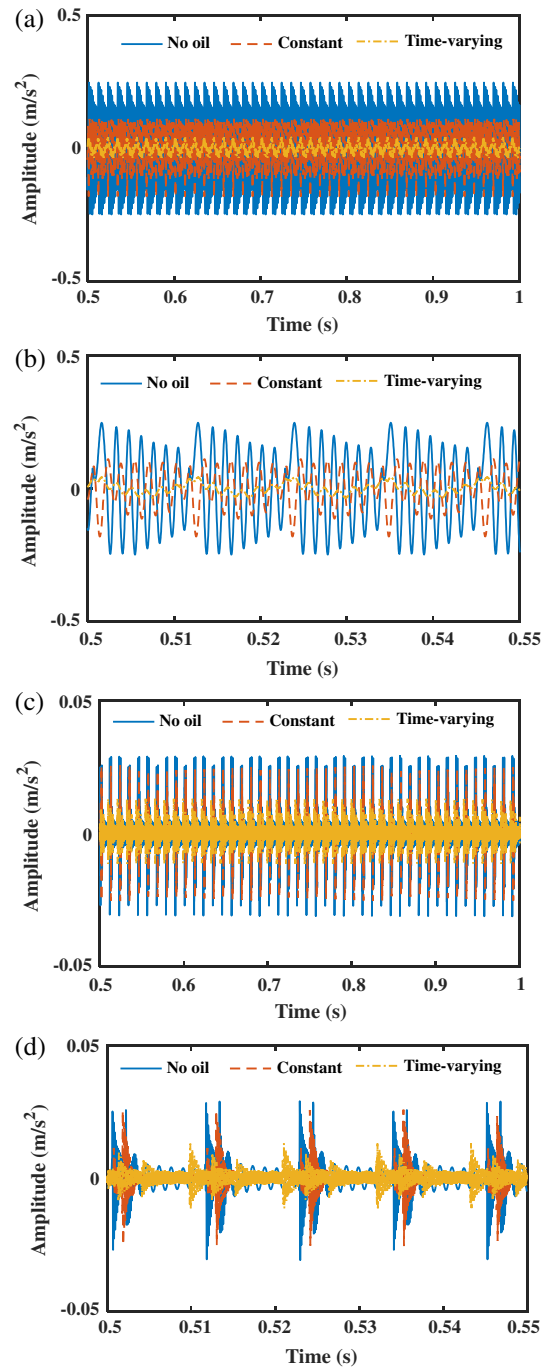

Fig. 9. Bearing vibration responses: (a, b) waveform of inner race and (c, d) outer race.

film are analysed. The working conditions for simulation study are listed in Table V.

Figures 12 and 13 depicts the thickness/stiffness of oil film at the centre of the load distribution under the influence of speed, and load, respectively.

From Fig. 12, the minimum oil film thickness between balls and inner/outer ring increases with the rotating speed, and the minimum oil film thickness between balls and outer ring is thicker than that between balls and inner ring. On the contrary, the oil film stiffness between the rolling elements and the inner/outer rings decreases with the increase of the rotational speed, and the oil film stiffness between the balls and the inner ring is larger.
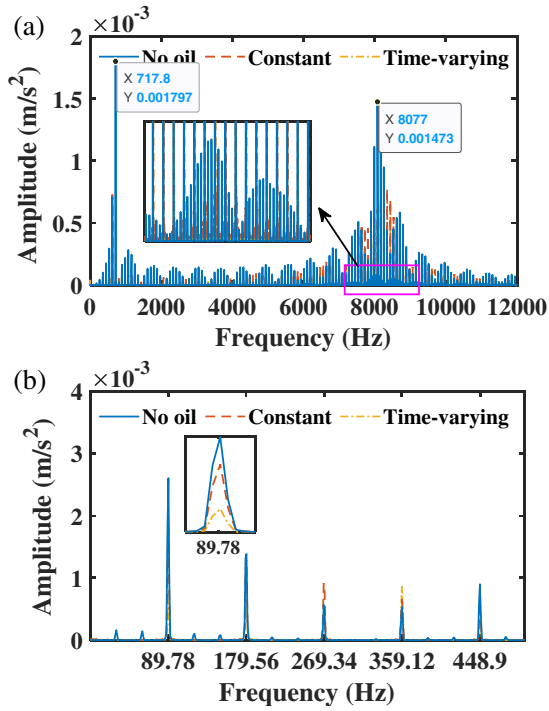
(a)

(b)

Fig. 10. Spectra analysis of outer race: (a) FFT spectrum and (b) envelope spectrum of frequency band [6000 Hz 10000 Hz].

Table IV   Characteristic frequencies of bearing 6206

Rotational speed (rpm)	BPFO (Hz)	BPFI (Hz)	BSF (Hz)	CF (Hz)
1500	89.78	135.22	59.37	9.98

From Fig. 13, the oil film thickness between the rolling balls and the inner/outer shows downtrend with the increase of load, while the oil film stiffness between the balls and the inner/outer rings shows uptrend with the increase of the load.

To investigate the influence of speed and load on bearing vibration, simulation under different working condition was carried out and RMS of the acceleration was calculated. Fig. 14 depicts RMS values under different working condition as shown in Table V. As can be seen, on general, the vibration RMS shows uptrends with the increase of speed and load.
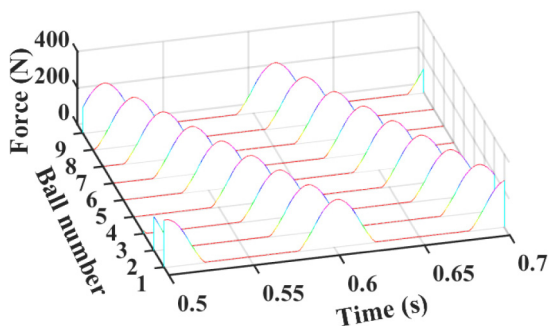

Fig. 11. Dynamic force during the operation.

Table V   Working conditions for simulation study

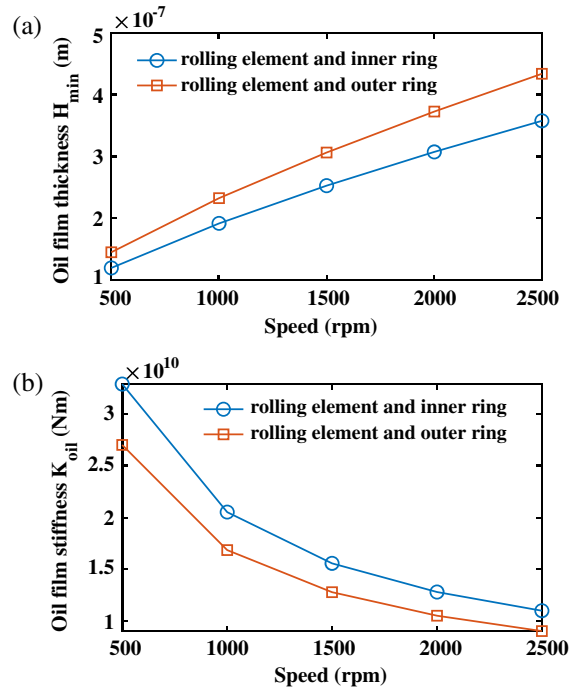| Description	Value
Speed (rpm)	500,1000,1500,2000,2500
Load (N)	100,200,300,400,500
Viscosity ($Pa \cdot s$)	0.2 (40°C)

(a)

(b)

Fig. 12. Relationship between the oil film thickness and speed (load is 500 N).
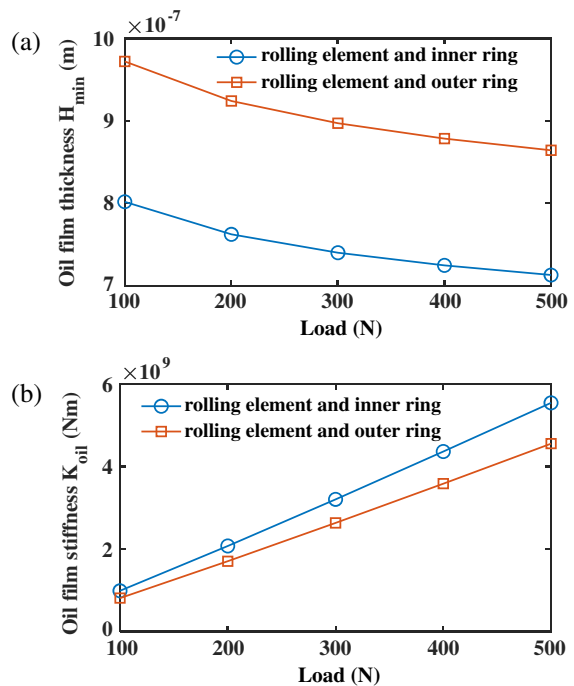
(a)

(b)

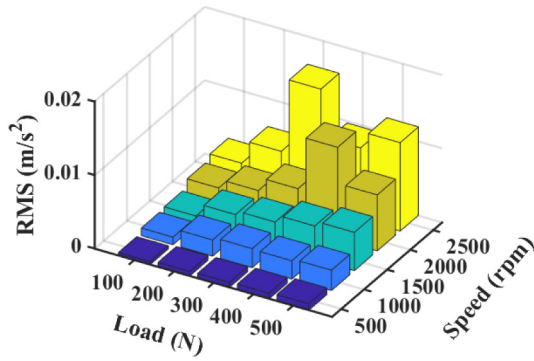**Fig. 13.** Relationship between the film stiffness and load (speed is 1500 rpm).

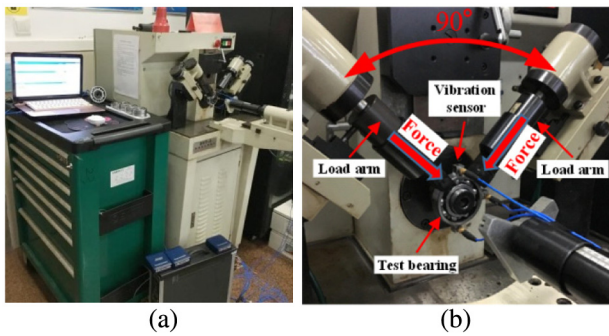**Fig. 14.** Vibration RMS under different working conditions (viscosity is $0.2Pa \cdot s$).

Fig. 15. Test facilities: (a) bearing test rig, (b) tested bearing and load arm.

V. VERIFICATION

A. EXPERIMENT SETTINGS

To verify the proposed bearing vibration model and the effect of oil film, an experiment is carried out on a bearing test rig (BVT-5). The bearing test rig contains a dabber, two load arms and a power transmission device, as shown in Fig. 15. The test bearing is deep groove ball bearing 6206 with clearances of C3. The angle between two load arms is 90° and each arm has two levels of load, i.e., 150 N and 300 N. Vehicle gear oil (85 W/90 GL-5) was selected as the lubrication oil. The vibration data was measured at the time when bearing works steadily after 30 minutes. The working conditions are listed in Table VI. Firstly, effect of oil film on vibrations is verified in the experiment. Secondly, the influence of speed and load on vibration is verified.

B. COMPARISONS BETWEEN SIMULATION AND EXPERIMENT

The state of oil starved is taken as the baseline and control group, while the state with rich lubrication oil is the treatment group. To correspond to the simulation, state

Table VI Working conditions for experiment study

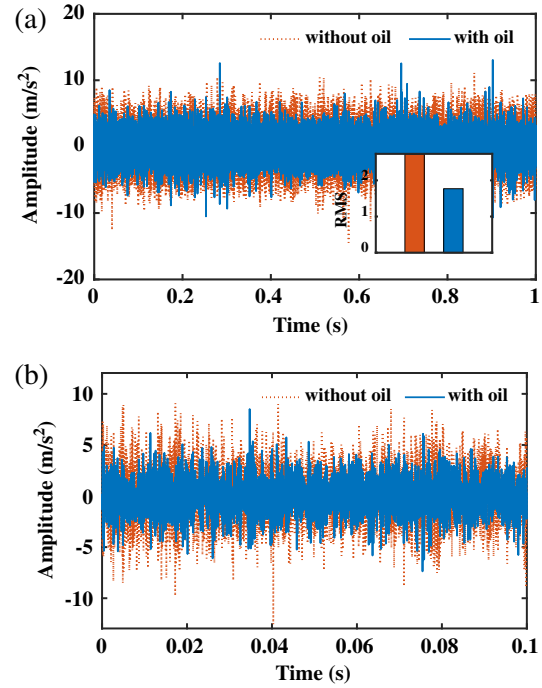| Description	Value
Speed (rpm)	500, 1000, 1500
Total load (N)	212 ($150\sqrt{2}$), 424 ($300\sqrt{2}$)
Oil viscosity ($Pa \cdot s$)	0.1743 (40°C)

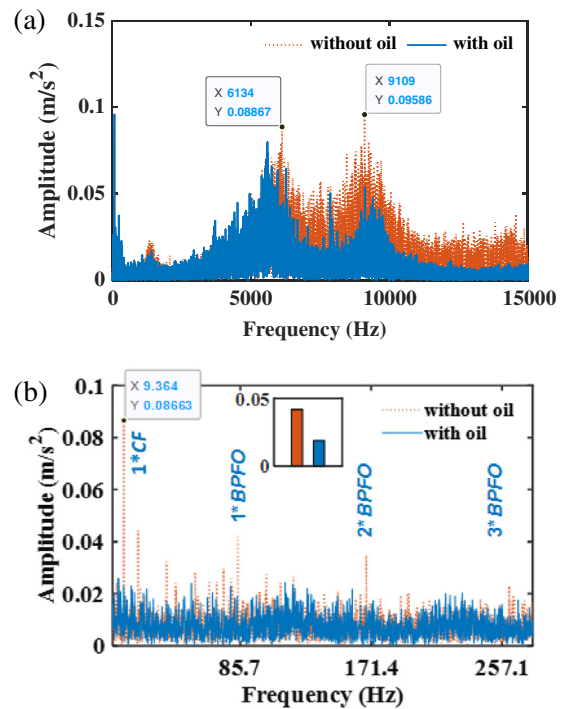**Fig. 16.** Vibration responses on time domain: (a) waveform and (b) its enlargement.

Fig. 17. Vibration responses in the frequency domain: (a) FFT spectrum and (b) envelope spectrum in the frequency band [6000 Hz 10000 Hz].

of oil starved is denoted as 'without oil' and state of oil rich is denoted as 'with oil'. Time domain waveform, FFT spectrum and envelope spectrum are shown in Figs. 16 and 17.
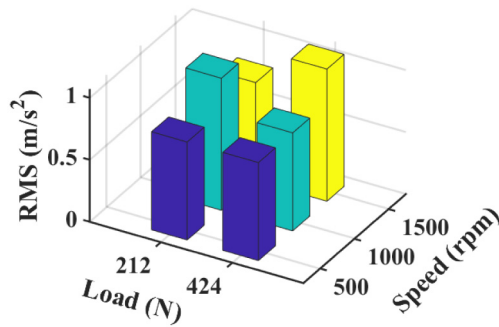
Fig. 18. RMS of vibration under different speed and load.

From Fig. 16, when oil film is taken in account, the vibration is lower on amplitude than without oil film from the waveform and RMS. The effect of oil film on vibration reduction is consistent with simulation, which verifies the reasonability of the method of considering time-varying oil characteristics in the bearing vibration model.

From the envelope spectrum, it can be found that BPFO is dominant, which is consistent with the simulation and verified the reasonability of the proposed model considering oil film.

To verify the influence of speed and load on vibrations, RMS values were calculated, as shown in Fig. 18.

As can be seen, the vibration level shows largely an uptrend with the increase of speed and load except the condition of 1500 rpm and 212 N. Even though the measured data is limited, the result shows good consistency with the simulation, which provides evidence for the reasonability of the improved bearing dynamic model.

VI.　CONCLUSIONS

This paper develops a bearing dynamic modelling method considering the time-varying characteristics of oil film and a fast calculation method for the oil film thickness and stiffness is proposed during the numerical solving process based on load distribution. Vibration responses analyses are carried out from time domain and frequency domain based on a thirteen-DOF nonlinear bearing model. Through the model and the analysis, it finds that whether considering oil film or not, the bearing characteristic frequency, BPFO, is dominant, due to the ball pass through the outer race plays a vital role to the bearing vibration during the operation. Specially, when oil film is included, the vibration is lower on amplitude than without oil film from both time domain and frequency domain. The oil film thickness increases with the speed, while decreases with load. The oil film stiffness shows the opposite result, decreasing with speed and increasing with load. On general, the vibration RMS shows uptrends with the increase of speed and load. An experiment was designed on a bearing test rig. The result is consistent with the simulation analysis about the effect of oil films and vibration responses under different working conditions, which verified the reasonability of the improved bearing vibration model and method for considering oil film in the model.

In the future, the damping coefficient will be studied from the shear action of oil and included into the vibration model. Besides, the when waviness appears on raceways, the thickness of the oil film will be affected by morphology

characteristics of raceway. Therefore, bearing waviness will be considered in future study.

CONFLICT OF INTEREST STATEMENT

The authors declare no conflicts of interest.

References

[1] R. B. Randall, "Detection and diagnosis of incipient bearing failure in helicopter gearboxes," *Eng. Fail. Anal.*, vol. 11, no. 12, pp. 177–190, 2004.

[2] Y. Xu, D. Zhen, J. X. Gu et al., "Autocorrelated envelopes for early fault detection of rolling bearings," *Mech. Syst. Signal Process.*, vol. 146, p. 106990, 2021.

[3] J. Guo, H. Zhang, D. Zhen et al., "An enhanced modulation signal bispectrum analysis for bearing fault detection based on non-Gaussian noise suppression," *Measurement*, vol. 151, p. 107240, 2020.

[4] T. A. Harris, "An analytical method to predict skidding in high speed roller bearings," *Asle Trans.*, vol. 9, no. 3, pp. 229–241, 1966.

[5] T. A. Harris, "An analytical method to predict skidding in thrust-loaded, angular-contact ball bearings," *J. Lubr. Technol.*, vol. 93, no. 1, pp. 17–23, 1971.

[6] P. K. Gupta, "Transient ball motion and skid in ball bearings," *J. Lubr. Technol.*, vol. 97, no. 2, pp. 261–269, 1975.

[7] C. R. Meeks and L. Tran, "Ball bearing dynamic analysis using computer methods-part I: analysis," *J. Tribol.*, vol. 118, no. 1, pp. 52–58, 1996.

[8] H. Cao, L. Niu, S. Xi, et al, "Mechanical model development of rolling bearing-rotor systems: a review," *Mech. Syst. Signal Process.*, vol. 102, pp. 37–58, 2018.

[9] J. Liu and Y. Shao, "Overview of dynamic modelling and analysis of rolling elements bearings with localized and distributed faults," *Nonlinear Dyn.*, vol. 93, no. 4, pp. 1765–1798, 2018.

[10] J. Liu and Y. Shao, "Dynamic modeling for rigid rotor bearing systems with a localized defect considering additional deformations at the sharp edges," *J. Sound Vib.*, vol. 398, pp. 84–102, 2017.

[11] J. Liu, X. Li, S. Ding et al., "A time-varying friction moment calculation method of an angular contact ball bearing with the waviness," *Mech. Mach. Theory*, vol. 148, p. 103799, 2020.

[12] M. Xu, G. Feng, Q. He et al., "Vibration characteristics of rolling elements bearings with different radial clearances for condition monitoring of wind turbine," *Appl. Sci.*, vol. 10, p. 4731, 2020.

[13] M. Xu, Y. Han, X. Sun et al., "Vibration characteristics and condition monitoring of internal radial clearance within a ball bearing in a gear-shaft-bearing system," *Mech. Syst. Signal Process.*, vol. 165, p. 108280, 2022.

[14] Y. H. Wijnant, J. A. Wensing, G. C. Nijen et al., "The influence of lubrication on the dynamic behaviour of ball bearings," *J. Sound Vib.*, vol. 222, no. 4, pp. 579–596, 1999.

[15] M. Sarangi, B. C. Majumdar, and A. S. Sekhar, "On the dynamics of elastohydrodynamic mixed lubricated ball

bearings. Part I: formulation of stiffness and damping coefficients," *Proc. Inst. Mech. Eng., Part J: J. Eng. Tribol.*, vol. 219, no. 6, pp. 411–421, 2006.

[16] M. Sarangi, B. C. Majumdar, and A. S. Sekhar, "On the dynamics of elastohydrodynamic mixed lubricated ball bearings. Part II: non-linear structural vibration," *Proc. Inst. Mech. Eng., Part J: J. Eng. Tribol.*, vol. 219, no. 6, pp. 423–433, 2006.

[17] Y. Zhang, X. Wang, X. Yan et al., "Dynamic behaviors of the elastohydrodynamic lubricated contact for rolling bearings," *J. Tribol.*, vol. 135, no. 2, p. 021501, 2013.

[18] A. Hajishafiee, A. Kadiric, S. Ioannides, and D. Dini, "A coupled finite-volume CFD solver for two-dimensional elasto-hydrodynamic lubrication problems with particular application to rolling elements bearings," *Tribol. Int.*, vol. 109, pp. 258–273, 2017.

[19] X. Cui, F. Meng, D. Kong et al., "Thermal elastohydrodynamic lubrication analysis of deep groove ball bearing," *Ind. Lubr. Tribol.*, vol. 70, no. 7, pp. 1282–1293, 2018.

[20] L. Bizarre, F. Nonato, and K. L. Cavalca, "Formulation of five degrees of freedom ball bearing model accounting for the nonlinear stiffness and damping of elastohydrodynamic point contacts," *Mech. Mach. Theory*, vol. 124, pp. 179–196, 2018.

[21] J. Wu, L. Wang, T. He, et al., "Investigation on the angular contact ball bearings under low speed and heavy load with coupled mixed lubrication and quasi-dynamic analysis," *Lubr. Sc.*, vol. 32, no. 3, pp. 108–120, 2020.

[22] S. Jain and H. Hunt, "A dynamic model to predict the occurrence of skidding in wind-turbine bearings," *J. Phys.: Conf. Series*, vol. 305, no. 1, p. 012027, 2011.

[23] Y. Zhang, Y. Li, et al., "The influence of elastohydrodynamic lubrication on the stiffness of deep groove ball bearing," *J. Vibroeng.*, vol. 18, no. 7, pp. 4178–4192, 2016.

[24] J. Liu and Y. Shao, "An improved analytical model for a lubricated roller bearing including a localized defect with different edge shapes," *J. Vib. Control*, vol. 24, no. 17, pp. 3894–3907, 2017.

[25] Q. Han, X. Li, and F. Chu, "Skidding behavior of cylindrical roller bearings under time-variable load conditions," *Int. J. Mech. Sci.*, vol. 135, pp. 203–214, 2018.

[26] Z. Shi and J. Liu, "An improved planar dynamic model for vibration analysis of a cylindrical roller bearing," *Mech. Mach. Theory*, vol. 153, p. 103994, 2020.

[27] T.A. Harris and M.N. Kotzalas, *Rolling bearing analysis : advanced concepts of bearing technology*. Taylor & Francis, Boca Raton, USA, 2007.

[28] L. Nayak and K.L. Johson, "Pressure between elastic bodies having a slender area of contact and arbitrary profikes," *Int. J. Mech. Sci.*, vol. 21, no. 4, pp. 237–247, 1979.